Computational Materials Science 151 (2018) 231–239

Contents lists available at ScienceDirect

Computational Materials Science

journal homepage: www.elsevier.com/locate/commatsci

First-principles studies of effects of layer stacking, opposite atoms, and stacking order on two-photon absorption of two-dimensional layered silicon carbide

You-Zhao Lan

Institute of Physical Chemistry, Key Laboratory of the Ministry of Education for Advanced Catalysis Materials, College of Chemistry and Life Sciences, Zhejiang Normal University, Zhejiang, Jinhua 321004, China

ARTICLE INFO

Keywords:
Layer stacking
Opposite atoms
Stacking order
Two-photon absorption
Silicon carbide

ABSTRACT

Based on the first-principles calculations of monolayer, bilayer, and trilayer two-dimensional layered silicon carbides, we show that layer stacking, opposite atoms, and stacking order slightly influence the transverse two-photon absorption coefficient (β_a) but significantly change the longitudinal two-photon absorption coefficient (β_c). From monolayer to few-layer, the values of β_c exhibit large enhancement owing to the effect of layer stacking, which not only increases the two-photon absorptive pathways but also enlarges the contribution of a single two-photon absorptive pathway to β_c. The effect of opposite atoms leads to different β_c profiles owing to different van der Waals interactions. The effect of stacking order increases the number of allowed two-photon absorptive pathways from *ABA* to *ABC* stacking but would not change the magnitude of TPA coefficients. For the few-layer configurations, the interlayer TPA transition channels make significant contributions to the total TPA process. Finally, we also show that two-photon absorption spectra are more suitable than one-photon absorption spectra for identifying different two-dimensional layered silicon carbides in terms of line shape and peak positions.

1. Introduction

Two-dimensional layered silicon carbide (2D-SiC) has attracted significant attention in recent years in both theoretical and experimental studies [1–7]. Although 2D-SiC is very similar to graphene in geometry, they have different electronic properties. For instance, monolayer graphene is a metal with unusual two-dimensional Dirac-like electronic excitations [8], whereas monolayer 2D-SiC with 1:1 Si/C stoichiometry is a semiconductor with a large gap of 2.55 eV (based on density functional theory calculations [6,9,10]), which increases to approximately 4.0 eV (based on the many-body *GW* approximation calculations [1,11–14]). The monolayer 2D-SiC can be rolled up to form the silicon carbide nanotube which has intriguing hydrogen storage after doped by metal [15–17]. The monolayer 2D-SiC with other stoichiometries such as SiC_3, SiC_5, and SiC_7 has also attracted significant interest owing to its potential applications such as light-emitting diodes, solar cells, and gas sensors [9,18–20]. However, it is difficult to obtain isolated monolayer (ML) 2D-SiC, and so far, only ultrathin 2D-SiC flakes with a thickness of 0.5–1.5 nm have been obtained [4].

With an increase in the number of layers, many properties such as electronic structure and optical properties exhibit new features demonstrated in few-layer (FL) graphene and 2D-SiC. A tunable band gap in the range of 70–250 meV can be obtained for graphene by applying an external electric field perpendicular to the bilayer (BL) graphene plane [21,22]. A layer-number-dependent principal transition was observed in the infrared conductivity measurements [23] of FL graphene with the layer number up to 8. The stacking-order dependent transport property was observed in trilayer (TL) graphene with *ABA*- and *ABC*-stacking [24]. The interlayer oriented misalignment [25] leads to the energy-renormalization of low-energy spectra [26] and twist-angle-dependent spectra [27]. As for nonlinear optical absorption properties, graphene has notable two-photon absorption (TPA) performance [28–33]. For instance, ML circular graphene quantum dots were observed to have significantly greater TPA than conventional semiconductor quantum dots in the infrared spectrum [30]. A similar significantly enhanced TPA behavior was also observed in BL graphene compared with ML graphene in the visible and infrared range [33].

For 2D-SiC, from ML-SiC to FL-SiC, the linear optical excitonic absorption spectra changed owing to the presence of interlayer transitions or hoppings in FL-SiC [34,35], and a direct-to-indirect band gap transformation was observed in the *ABA*-stacked 2D-SiC. Notably, the interlayer-oriented misalignment in the FL-SiC results in an indirect-to-

E-mail address: lyzhao@zjnu.cn.

https://doi.org/10.1016/j.commatsci.2018.04.058
Received 22 January 2018; Received in revised form 2 April 2018; Accepted 24 April 2018
0927-0256/ © 2018 Elsevier B.V. All rights reserved.

direct transition in the band structure [5]. In addition to the layer-number, stacking-order, and oriented-misalignment-dependent properties, the FL-SiC exhibits the opposite-atoms-dependent property because there could be different opposite atoms (i.e., SiC, CC, and SiSi) between layers. It has been shown that the BL-SiC with different opposite atoms has distinct structural stabilities and electronic structures [36,37], which leads to different optical properties.

In this work, we investigate the effects of layer stacking, opposite atoms, and stacking order on the TPA properties of 2D-SiC with 1:1 Si/C stoichiometry based on the Bernal-stacked (*ABA*-stacked) FL-SiC, *AB*- and *AA*-stacked BL-SiC, and *ABA*- and *ABC*-stacked TL-SiC configurations. The band structures and optical matrix elements for calculating the TPA coefficient (β) in the second-order perturbation theory [38] were obtained by using the all-electron full potential linearized augmented plane wave (FP-LAPW) method [39] with the modified Becke–Johnson (mBJ) exchange potential [40] combined with the local-density approximation (LDA)-based Perdew and Wang (PW) correlation potential [41]. To understand the physical origin of the three effects influencing the TPA of 2D-SiC, we extract the main single-particle transition channels of TPA by tracing the sum-over-states (SOS) process. In Section 2, we provide the computational details of geometry, band structures, and optical properties. In Section 3, we discuss the effects of layer stacking, opposite atoms, and stacking order on the TPA properties of 2D-SiC. Finally, the conclusions are presented in Section 4.

2. Computational details

2.1. Geometry

The crystal structures of all the two-dimensional layered SiC configurations are shown in Fig. 1. ML-SiC has a planar structure with D_{3h} symmetry [4,6,42]. For FL-SiC, to investigate the effects of opposite atoms and stacking order on TPA, we considered *AA*- and *AB*-stacked BL-SiC and *ABA*- and *ABC*-stacked TL-SiC configurations. Hereafter, *A*, *AA* or *AB*, and *ABA* or *ABC* also indicate ML-, BL-, and TL-SiC, respectively. All the configurations were optimized by using the density functional theory within the generalized gradient approximation (GGA) of the Perdew–Burke–Ernzerhof (PBE) functional [43] combined with the pseudopotential plane wave method, as implemented in the CASTEP code [44] of Material Studio 4.0. A *k*-point mesh of 10 × 10 × 1, force threshold of 0.01 eV/Å, and stress threshold of 0.02 GPa were used for the optimizations. The relaxation of the unit cell was included in the optimization. The optimized interlayer distances are listed in Table 1. As conventional DFT cannot treat the interlayer van der Waals interaction effectively, the semi-empirical dispersion correction based on the Tkatchenko and Scheffler (TS) scheme [45] was used in the optimizations. Based on the DFT-TS correction, the optimized interlayer distance of *AB*-SiC is 3.46 Å very close to the measured interlayer

Table 1
Opposite atoms at the positions of 1, 2, 3, and 4 (Fig. 1), interlayer distances (d_1 and d_2), and direct (E_g^d) and indirect (E_g^i) gaps of all configurations. The E_g^i is defined as the energy difference between the valence band maximum and the conduction band minimum in the whole band structure, while the E_g^d is defined as the smallest energy difference between the valence band top and conduction band bottom at the same *k* point. The structure is intrinsically indirect for $E_g^d > E_g^i$ and direct for $E_g^d = E_g^i$.

	Position				Distance (Å)		Gap (eV)	
Configurations	1	2	3	4	d_1	d_2	E_g^i	E_g^d
A	C						3.93	4.09
AA-CC	C	C			3.94		3.05	3.22
AA-SiC	Si	C			2.19		3.25	4.13
AB-SiC	Si	C			3.46		3.33	3.62
AB-CC	C	C			3.84		3.04	3.55
AB-SiSi	Si	Si			3.39		2.66	2.69
ABA-SiCSi	Si	C	Si		3.44	3.44	3.21	3.40
ABA-CSiC	C	Si	C		3.45	3.45	3.34	3.60
ABC-CSiCC	C	Si	C	C	3.44	3.82	2.84	3.32
ABC-CSiCSi	C	Si	C	Si	3.46	3.45	2.82	3.23
ABC-SiCSiSi	Si	C	Si	Si	3.41	3.38	2.22	2.22
ABC-SiSiCC	Si	Si	C	C	3.36	3.79	2.27	2.27

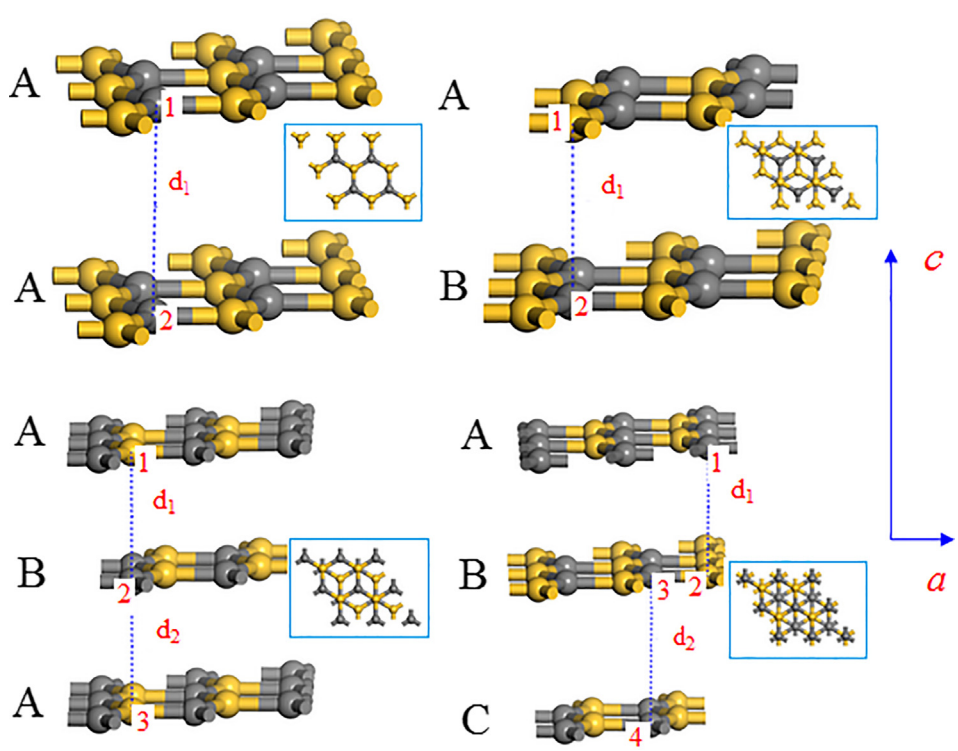

Fig. 1. Side-view of structures of *A*-, *AA*-, *AB*-, *ABA*-, and *ABC*-stacked two-dimensional layered SiC. The arrows indicate the lattice vectors *a* and *c*. Atoms at the positions of 1, 2, 3, and 4 and interlayer distances d_1 and d_2 are listed in Table 1. Insets (rounded by rectangle) are the corresponding top-views of the structures.

Download English Version:

https://daneshyari.com/en/article/7957319

Download Persian Version:

https://daneshyari.com/article/7957319

Daneshyari.com